Macular Ganglion Cell Inner Plexiform Layer Thinning in Patients with Visual Field Defect that Respects the Vertical Meridian

Hye-Young Shin, Chan Kee Park

Abstract—*Background*: To compare the thinning patterns of the ganglion cell-inner plexiform layer (GCIPL) and peripapillary retinal nerve fiber layer (pRNFL) as measured using Cirrus high-definition optical coherence tomography (HD-OCT) in patients with visual field (VF) defects that respect the vertical meridian.

Methods: Twenty eyes of eleven patients with VF defects that respect the vertical meridian were enrolled retrospectively. The thicknesses of the macular GCIPL and pRNFL were measured using Cirrus HD-OCT. The 5% and 1% thinning area index (TAI) was calculated as the proportion of abnormally thin sectors at the 5% and 1% probability level within the area corresponding to the affected VF. The 5% and 1% TAI were compared between the GCIPL and pRNFL measurements.

Results: The color-coded GCIPL deviation map showed a characteristic vertical thinning pattern of the GCIPL, which is also seen in the VF of patients with brain lesions. The 5% and 1% TAI were significantly higher in the GCIPL measurements than in the pRNFL measurements (all *P* < 0.01).

Conclusions: Macular GCIPL analysis clearly visualized a characteristic topographic pattern of retinal ganglion cell (RGC) loss in patients with VF defects that respect the vertical meridian, unlike pRNFL measurements. Macular GCIPL measurements provide more valuable information than pRNFL measurements for detecting the loss of RGCs in patients with retrograde degeneration of the optic nerve fibers.

Keywords—Brain lesion, Macular ganglion cell-Inner plexiform layer, Spectral-domain optical coherence tomography.

I. INTRODUCTION

GENERALLY, damage to the human central nervous system leads to retrograde *trans*-synaptic degeneration [1]-[4]. Optical coherence tomography (OCT) studies have revealed peripapillary retinal nerve fiber layer (pRNFL) loss in patients with various types of cerebral damage, including damage to the frontal, parietal, temporal, and occipital lobes [1], [2], [5], [6]. However, the ganglion cells on the temporal retina of the fovea primarily send their exons to the superior and inferior sectors of the optic nerve head (ONH), including the temporal sector. In additions, the axons of the ganglion cells on the nasal retina of the fovea are located in all sectors the ONH. Therefore, pRNFL analysis makes it difficult to clarify the pattern of retinal ganglion cell (RGC) loss due to superimposed axons around the ONH.

Recent RTVue analyses demonstrated that ganglion cell complex (GCC) measurements showed a unique pattern of GCC thinning in patients with homonymous hemianopia [7], [8]. However, the RTVue analysis measures the thickness of the three inner layers (ganglion cell layer, inner plexiform layer, and RNFL). Since the thickness of the axons from RGCs in the temporal retina makes it difficult to identify RGC loss the in nasal retina clearly, GCC analysis has the same limitation as pRNFL analysis. Unlike GCC analysis, macular ganglion cell-inner plexiform layer (GCIPL) analysis measured by the Cirrus OCT macular scan excludes the RNFL. The macular GCIPL comprises ganglion cell layer (GCL), which is composed of cell bodies of RGCs, and the inner plexiform layer (IPL), which contains the RGC dendrites. Therefore, we assumed that macular GCIPL could clearly visualize the vertical pattern of RGC loss in the retinas of patients with visual field (VF) defects that respect the vertical meridian.

Homonymous hemianopia (HH) results from various lesions involving the retrochiasmal visual pathways [9], [10]. Most publications report GCC thinning in complete homonymous hemianopia (HH) [7], [8]; however, incomplete HH is more common than complete HH [9]. Incomplete HH is defined as a homonymous VF defect that respects the vertical meridian with some normal VF in the affected hemifield, this can include HH with macular sparing, partial HH, homonymous quadrantanopia, homonymous scotomatous defects, homonymous sectoranopia, and unilateral loss of the temporal crescent [9]. In one study, 11 of 12 patients with HH who continued to drive had incomplete HH [11]. This suggests that incomplete HH does not severely affect the activities of daily life and sometimes can be overlooked. However, it is important to identify patients with incomplete HH because this suggests a brain lesion, even if there are no neurological symptoms. Macular GCIPL analysis that can detect RGC loss earlier will be valuable in patients with suspicious VF defects. This study compares the pattern and extent of GCIPL and RNFL thinning in patients with VF defects that respect the vertical meridian.

II. PATIENTS AND METHODS

This cross-sectional study retrospectively enrolled 20 eyes of 11 patients with VF defects that respect the vertical meridian from the clinical database at the glaucoma clinic of Seoul St. Mary's Hospital, Korea, between April 2012 and October 2013. This study was conducted in accordance with

Hye Young Shin is with the College of Medicine, Catholic University of Korea, Korea, Republic of (e-mail: antares78@empal.com).

the Declaration of Helsinki and with the approval of the hospital Institutional Review Board.

Upon initial evaluation, each participant underwent a comprehensive ophthalmologic examination, including a review of medical and ocular histories, measurement of best-corrected visual acuity, slit-lamp biomicroscopy, Goldmann applanation tonometry, gonioscopic examination, dilated fundoscopic examination, stereoscopic optic disc photography, red-free RNFL photography, Spectral domain(SD)-OCT scanning (Cirrus HD-OCT; Carl Zeiss Meditec, Dublin, CA) and visual field examination, using the 24–2 Swedish Interactive Threshold Algorithm (SITA) standard program (Humphrey Visual Field Analyzer; Carl Zeiss-Meditec, Inc., Dublin, CA). Participants included in this study met the following criteria: best corrected visual acuity of 20/30 or better, a spherical equivalent between -6.0 and +4.0 diopters and a cylinder correction within ±3.0 diopters, the presence of a normal anterior chamber and open-angle on slit-lamp and gonioscopic examinations, and reliable visual field test results. The reliability was defined as fixation loss ≤ 20%, false-positive ≤15%, and false-negative ≤15%. Subjects with a history of any retinal disease, such as diabetic macula edema, epiretinal membrane, foveoschisis, and age-related macular degeneration, which can affect macular thickness, or ocular trauma or surgery with the exception of uncomplicated cataract surgery, were excluded. Incomplete HH was defined as having homonymous VF defects that respect the vertical meridian and a partially normal VF in the affected hemifield, as confirmed on at least two reliable VF examinations. Patients with partial HH, homonymous quadrantanopia, or homonymous scotomatous defects were enrolled in this study.

A. Optical Coherence Tomography

Spectral domain-OCT imaging was performed using a Cirrus high-definition (HD) -OCT with the ver. 6.0 software. For GCIPL analysis, three-dimensional macular cube OCT data were obtained using the macular cube 512 × 128 scan mode. The average, minimum, and sectoral (superotemporal, superior, superonasal, inferonasal, inferior, inferotemporal) thicknesses of the GCIPL were measured in an elliptical annulus (vertical outer radius 2.0 mm, horizontal outer radius 2.4 mm). The GCA algorithm compares the values with an internal normative database, and generates thickness and color-coded deviation maps, and a significance map to match GCIPL thickness, with values within the normal range in green ($P = 5\% – 95\%$), borderline values in yellow ($1\% < P < 5\%$), and values outside the normal range in red ($P < 1\%$). Details of the manner in which GCIPL thickness measurements are conducted have been given elsewhere [12], [13]. Using SD-OCT, the RNFL thickness was measured in the optic disc cube 200 × 200 scan mode. The Cirrus HD-OCT algorithm calculates the overall average RNFL thickness, RNFL thickness of each quadrant, and individual RNFL thickness of all 12 clock-hour sectors and generates thickness, color-coded deviation, and significance maps. Images with signal strength <6 or algorithm segmentation failure and those with blinking artifacts or visible eye motion were considered poor quality and discarded.

We divided the retina into four quadrants that match the VF quadrants. We also divided the six GCIPL sectors into four corresponding areas and the pRNFL sectors into superior and inferior hemifield pRNFL sectors. The superior hemifield pRNFL sectors were defined as the region containing the sectors in clock-hours 9 to 12 and 1 to 3 and the inferior hemifield pRNFL sectors were the sectors at clock-hours 3 to 9. We compared the superotemporal and superior GCIPL macular sectors and superior hemifield pRNFL sectors of the right eye and the superior and superonasal GCIPL sectors and superior hemifield pRNFL sectors of the left eye in patients with a left inferior quadrant VF defect. In patients with a left superior quadrant VF defect, we compared the inferotemporal and inferior GCIPL macular sectors and inferior hemifield pRNFL sectors of the right eye and the inferior and inferonasal GCIPL sectors and inferior hemifield pRNFL sectors of the left eye.

To exclude as many axons that are superimposed on the ONH as possible, we subdivided the pRNFL sectors into superior arcuate, inferior arcuate, superior non-arcuate, and inferior non-arcuate subfield pRNFL sectors. The superior arcuate subfield comprised the region at clock-hours 10 to 1 and the superior non-arcuate subfield combined the sectors at clock-hours 2, 3, 9, and 10. We compared the superotemporal and superior GCIPL macular sectors and superior arcuate subfield pRNFL sector of the right eye in patients with left inferior quadrant VF defects because the thinning of retinal nerve fibers was seen predominantly in the arcuate area among the superior hemifield pRNFL sectors, although retinal nerve fibers from the nasal retina remain.[2] The superior and superonasal GCIPL sectors and superior non-arcuate subfield pRNFL sector of the left eye were compared because there was total loss of fibers in the nasal region and partial loss of fibers in the temporal region of the optic disc (Fig. 1) [2]. In patients with left superior quadrant VF defects, we compared the inferotemporal and inferior GCIPL macular sectors and inferior arcuate subfield pRNFL (clock-hours 5 to 8) sectors of the right eye. The inferior and inferonasal GCIPL sectors and inferior non-arcuate subfield pRNFL sectors (clock-hours 3, 4, 8, and 9) of the left eye were compared.

The 5% thinning area index (TAI) was calculated as the proportion of abnormally thin sectors (below normal at the 5% probability level) within the corresponding area. Similarly, the 1% TAI was calculated as the proportion of abnormally thin sectors at the 1% probability level.

B. Statistical Analyses

Wilcoxon's signed-rank test was used to compare the 5% and 1% TAI between the GCIPL and pRNFL measurements. All reported P values are two-sided, and differences at a level of $P < 0.05$ were considered to be statistically significant. The Statistical Package for the Social Sciences version 18.0 (SPSS Inc., Chicago, IL) was used for all statistical analyses.
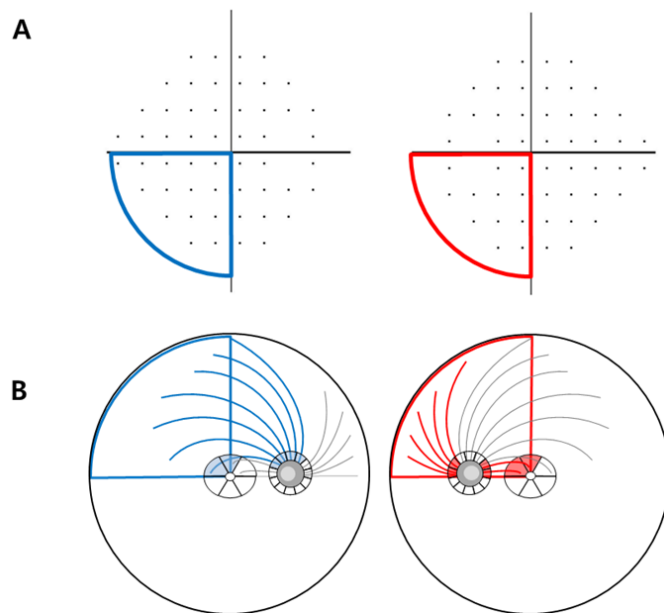
Fig. 1 Visual field (VF) of the Humphrey field analyzer Swedish interactive threshold algorithm 24-2 paradigm, ganglion cell–inner plexiform layer (GCIPL) and peripapillary retinal nerve fiber layer (pRNFL) thickness measurements using Cirrus high-definition optical coherence tomography. **A**, The VF pattern deviation map showing the left inferior quadrant marked with blue and red lines. **B**, In the right eye, the blue sectors were analyzed: the superotemporal and superior GCIPL macular sectors and superior arcuate subfield pRNFL sectors (at clock-hours 10 to 1). In the left eye, the red sectors were analyzed: the superior and superonasal GCIPL sectors and superior non-arcuate subfield pRNFL sectors (at clock-hours 2, 3, 9, and 10).

TABLE I
PATIENT DEMOGRAPHICS

Case	Gender	Age	Cause	Side	Location of VFD
1	Female	24	Brain surgery due to craniopharyngioma	OD	Lt. inferior Q
				OS	Lt. inferior Q
2	Female	31	Right cerebral infarction	OD	Lt. superior Q
				OS	Lt. superior Q
3	Female	67	Right cerebral infarction	OD	Lt. inferior Q
				OS	Lt. inferior Q
4	Female	68	Presumed sequele of neurocycticercosis	OS	Rt. inferior Q
5	Male	24	Brain surgery due to epilapsy	OD	Rt. superior Q
				OS	Rt. superior Q
6	Male	34	Brain surgery due to hydrocephalus	OD	Rt. superior Q
				OS	Rt. superior Q
7	Male	39	Left cerebral infarction	OD	Rt. inferior Q
				OS	Rt. inferior Q
8	Male	62	Brain surgery due to glioblastoma	OD	Lt. superior Q
9	Male	65	Cerebral hemorrhage	OD	Lt. inferior Q
				OS	Lt. inferior Q
10	Male	75	Cerebral hemorrhage	OD	Lt. superior Q
				OS	Lt. superior Q
11	Male	78	Right cerebral infarction	OD	Lt. superior Q
				OS	Lt. superior Q

VFD = visual field defect; Q = quadrant

TABLE II
COMPARISON OF THE THINNING AREA INDEX BETWEEN THE GCIPL AND pRNFL MEASUREMENTS

	GCIPL	pRNFL		P value*	P value†
		Hemifield	Subfield		
5% Thinning Area Index	87.50±22.21	30.71±19.81	33.75±24.70	<0.001	<0.001
1% Thinning Area Index	62.50±45.52	17.14±16.45	19.17±24.35	<0.001	<0.001

Data are presented as means ± standard deviation.
*Comparison between GCIPL and hemifield pRNFL by Wilcoxon's signed-ranks test
†Comparison between GCIPL and subfield pRNFL by Wilcoxon's signed-ranks test
GCIPL = ganglion cell–inner plexiform layer; pRNFL = peripapillary retinal nerve fiber layer
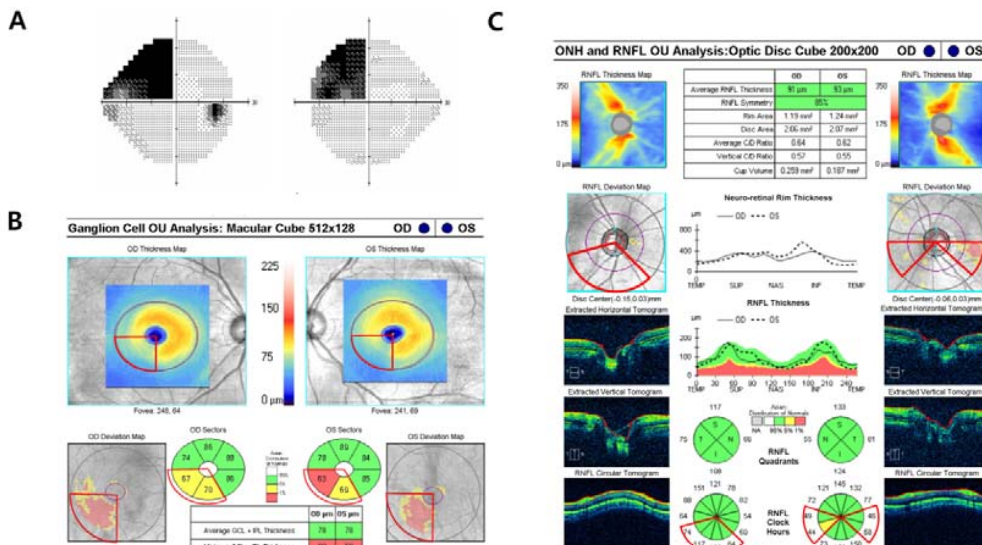
Fig. 2 Images from a patient (case 10) with left superior visual field defects. **A**, Standard automated perimetry showing left superior homonymous scotomatous defects. **B**, Cirrus OCT macular cube scan images show a decrease in GCIPL thickness in all of the corresponding sectors in both eyes. The vertical pattern of RGC loss is clearly visualized in the color-coded GCIPL deviation map. **C**, Cirrus OCT optic nerve head images show that pRNFL thickness in the corresponding sectors is within the normal range in the right eye, although the pRNFL thicknesses in one of four sectors were outside the normal range in the left eye. The sectors within the red line correspond to the left superior VF quadrant. The GCIPL thinning reflects RGC loss more clearly than RNFL thinning within the affected retina. GCIPL = ganglion cell–inner plexiform layer; pRNFL = peripapillary retinal nerve fiber layer; OCT = optical coherence tomography
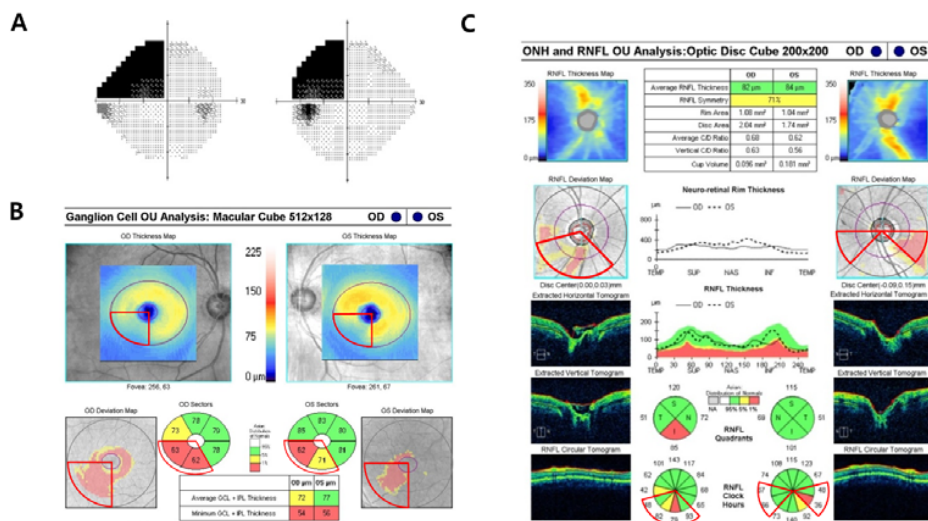
Fig. 3 Images from a patient (case 11) with left superior visual field defects. **A**, Standard automated perimetry showing left superior homonymous scotomatous defects. **B**, Cirrus OCT macular cube scan images show a decrease in GCIPL thickness in all of the corresponding sectors in both eyes. The vertical pattern of RGC loss is clearly visualized in the color-coded GCIPL deviation map. **C**, Cirrus OCT optic nerve head images show that the pRNFL thicknesses in two of four sectors were outside the normal range in the right eye and the pRNFL thicknesses in one of four sectors were outside the normal range in the left eye. The GCIPL thinning reflects RGC loss more clearly than RNFL thinning within the affected retina. GCIPL = ganglion cell–inner plexiform layer; pRNFL = peripapillary retinal nerve fiber layer; OCT = optical coherence tomography

III. RESULTS

This study initially included 20 eyes from 11 patients who had incomplete homonymous hemianopia. Two eyes of two patients were excluded from further analysis because of unacceptable Cirrus-OCT scans quality. The subject characteristics are summarized in Table I.

The number of the eyes that had abnormal sectors within the corresponding region was greater with the macular GCIPL measurements (N=20) than the pRNFL measurements (N=15).

Table II shows the TAIs for the GCIPL and pRNFL measurements. The 5% and 1% TAIs were significantly higher in GCIPL sectors than in hemifield pRNFL sectors (87.50±22.21% vs. 30.71±19.81%, $P < 0.001$ and 62.50±45.52% vs. 17.14±16.45%, $P = 0.001$, respectively). Furthermore, the 5% and 1% TAIs were significantly higher in GCIPL sectors than in subfield pRNFL sectors (87.50±22.21% vs. 33.75±24.70%, $P < 0.001$ and 62.50±45.52% vs. 19.17±24.35%, $P = 0.001$, respectively).

IV. DISCUSSION

Several studies have detected retinal nerve fiber loss using optical coherence tomography (OCT) in humans with various types of cerebral damage [1], [2], [5]. However, the loss of RGCs in patients with incomplete HH has never been assessed using GCIPL measurements. In this study, we quantitatively compared the macular GCIPL and pRNFL thinning in the sectors corresponding to the affected visual fields in patients with VF defects that respect the vertical meridian. We demonstrated a characteristic thinning pattern of macular GCIPL thickness in patients with incomplete HH using a Cirrus OCT macular scan, unlike the pRNFL thickness measurement.

Table II shows that the 5% and 1% TAIs were significantly higher with the GCIPL measurements than the pRNFL measurements (all $P < 0.01$). This is likely because the axons from RGCs on the nasal and temporal sides of the fovea are superimposed around the ONH. Only axons from RGCs on the nasal side of the ONH were not mixed up. In addition, the Cirrus OCT measured the GCIPL thickness in an elliptical area around the fovea [12]. Since approximately 50% of the RGCs are concentrated within 4.5 mm of the fovea [14], thinning of the macular GCIPL can be better visualized topographically, compared to thinning of the RNFL. GCIPL analysis produced a color-coded deviation map, which enabled us to visualize the vertical pattern of GCIPL thinning, which is also seen in the VF examinations of patients with brain lesions. We found that pRNFL loss around the ONH was not always detected using Cirrus OCT, especially in patients with incomplete HH (Figs. 2 and 3). Macular GCIPL measurement proved a better tool than pRNFL measurement for visualizing the RGC loss.

Previous reports found GCC analysis to be superior to pRNFL for detecting optic nerve damage in patients with HH [7], [8]. However, GCC analysis has the same limitations as pRNFL, because the GCC thickness is the sum of the RNFL, ganglion cell, and inner plexiform layer thicknesses, unlike GCIPL thickness. The thickness of axons from RGCs in the temporal retina makes it difficult to identify RGC loss in the nasal retina clearly, because the axons from RGCs on both sides of fovea are superimposed around the ONH. In addition, the previous study using GCC analysis showed that the GCC thinning was more pronounced in the central retina, compared to the peripheral retina [8]. This may be partly because approximately 50% of the RGCs are concentrated within 4.5 mm of the fovea [14]. Therefore, the GCIPL thickness measured in central macular region using Cirrus OCT allows a more precise topographic analysis of the RGCs than the pRNFL and GCC thicknesses.

Incomplete HH is more common than complete HH.[9] In complete HH include HH with macular sparing, partial HH, homonymous quadrantanopia, homonymous scotomatous defects, homonymous sectoranopia, and unilateral loss of the temporal crescent [9]. A representative case with incomplete HH is shown in Fig. 2. While the pattern of pRNFL thinning was unclear, the vertical pattern of GCIPL thinning was obvious. Therefore, we believe that macular GCIPL measurement is a sensitive method for detecting RGC loss in patients with VF defects suspected of being associated with brain lesions.

Traditionally, perimetry has been used to detect the loss of RGCs in patients with retrograde degeneration of the optic nerve fiber and the location of the VF defects has been used to localize the brain lesion approximately. In this study, we demonstrated that GCIPL measurement might be used to localize brain lesions more precisely than RNFL measurement. In patients with vertical pattern of GCIPL thinning, the brain lesions should be suspected although there were no neurologic symptoms yet.

In the previous studies, the time course of the retrograde degeneration has been demonstrated using RNFL measurements [1], [5]. Given that the changes of the RNFL thickness than GCIPL thickness do not reflect the retrograde degeneration well, there is the possibility that the retrograde degeneration might have been happen earlier than previously reported as. However, this possibility requires further validation studies.

This study had limitations. First, the sample size was relatively small. However, the differences between the GCIPL and pRNFL thickness measurements were statistically significant. Second, for sectoral comparisons, we used the GCIPL and pRNFL sectors pre-defined in the commercial software supplied with the Cirrus OCT. Therefore, the GCIPL sectors used for analysis do not match the quadrants of the retina topographically and the pRNFL sector would not match the retina quadrants perfectly because of superimposed axon fibers around the ONH. To our knowledge, however, this is the first study to compare GCIPL and pRNFL measurements quantitatively in patients with incomplete HH, in which the extent of the VF defect is milder than in complete HH. We also demonstrated that the color-coded GCIPL deviation map clearly illustrated the vertical pattern of GCIPL thinning.

In conclusion, macular GCIPL measurement using Cirrus-OCT could detect the characteristic vertical area of GCIPL thinning implying retrograde RGC loss in patients with VF defects that respected the vertical meridian, while the pattern of pRNFL thinning was not apparent. We recommend measuring the macular GCIPL in all patients with VF defects that respect the vertical meridian.

and take responsibility for the integrity of the data and the accuracy of the data analysis as well as the decision to submit for publication.

REFERENCES

[1] Jindahra P, Petrie A, Plant GT (2012) The time course of retrograde trans-synaptic degeneration following occipital lobe damage in humans. Brain 135: 534-541.

[2] Jindahra P, Petrie A, Plant GT (2009) Retrograde trans-synaptic retinal ganglion cell loss identified by optical coherence tomography. Brain 132: 628-634.

[3] Bridge H, Jindahra P, Barbur J, Plant GT (2011) Imaging reveals optic tract degeneration in hemianopia. Investigative ophthalmology & visual science 52: 382-388.

[4] Cowey A, Alexander I, Stoerig P (2011) Transneuronal retrograde degeneration of retinal ganglion cells and optic tract in hemianopic monkeys and humans. Brain 134: 2149-2157.

[5] Park HY, Park YG, Cho AH, Park CK (2013) Transneuronal Retrograde Degeneration of the Retinal Ganglion Cells in Patients with Cerebral Infarction. Ophthalmology 120: 1292-1299.

[6] Tatsumi Y, Kanamori A, Kusuhara A, Nakanishi Y, Kusuhara S, Nakamura M (2005) Retinal nerve fiber layer thickness in optic tract syndrome. Japanese journal of ophthalmology 49: 294-296.

[7] Kanamori A, Nakamura M, Yamada Y, Negi A (2013) Spectral-domain optical coherence tomography detects optic atrophy due to optic tract syndrome. Graefes Arch Clin Exp Ophthalmol 251: 591-595.

[8] Yamashita T, Miki A, Iguchi Y, Kimura K, Maeda F, Kiryu J (2012) Reduced retinal ganglion cell complex thickness in patients with posterior cerebral artery infarction detected using spectral-domain optical coherence tomography. Japanese journal of ophthalmology 56: 502-510.

[9] Zhang X, Kedar S, Lynn MJ, Newman NJ, Biousse V (2006) Homonymous hemianopias: clinical-anatomic correlations in 904 cases. Neurology 66: 906-910.

[10] Newman SA, Miller NR (1983) Optic tract syndrome. Neuro-ophthalmologic considerations. Arch Ophthalmol 101: 1241-1250.

[11] Gilhotra JS (2002) Homonymous Visual Field Defects and Stroke in an Older Population. Stroke 33: 2417-2420.

[12] Mwanza JC, Oakley JD, Budenz DL, Chang RT, Knight OJ, Feuer WJ (2011) Macular ganglion cell-inner plexiform layer: automated detection and thickness reproducibility with spectral domain-optical coherence tomography in glaucoma. Investigative ophthalmology & visual science 52: 8323-8329.

[13] Mwanza JC, Durbin MK, Budenz DL, Girkin CA, Leung CK, Liebmann JM, Peace JH, Werner JS, Wollstein G (2011) Profile and predictors of normal ganglion cell-inner plexiform layer thickness measured with frequency-domain optical coherence tomography. Investigative ophthalmology & visual science 52: 7872-7879.

[14] Curcio CA, Allen KA (1990) Topography of ganglion cells in human retina. The Journal of comparative neurology 300: 5-25.